

- kinks (see Fig. 3) reflects liquid-solid coexistence points at a given temperature and composition.
29. We may have observed the hemihydrate as well; however, it is favored at high  $p_{\text{H}_2\text{O}}/p_{\text{HNO}_3}$  ratios where ice nucleation tended to complicate metastable phase identification.
  30. R. Zhang, P. J. Wooldridge, J. P. D. Abbat, M. J. Molina, *J. Phys. Chem.* **97**, 7351 (1993); R. Zhang, thesis, Massachusetts Institute of Technology (1993).
  31. Our observations determine only the ratio  $l/m$  for different  $l - k$  observations (as with  $n$  in Eq. 3). We chose  $m = 1$ , implying 1:1  $\text{H}_2\text{SO}_4:\text{HNO}_3$  composition in the mixed hydrate, the simplest case.
  32. B. G. Koehler, A. M. Middlebrook, M. A. Tolbert, *Geophys. Res. Lett.* **97**, 8065 (1992).
  33. This  $\alpha$ -NAT phase was identified from slightly high  $K_{\text{HNO}_3 \cdot 3\text{H}_2\text{O}}$  values that were observed only during initial nucleation of NAT, usually converting to NAT overnight, consistent with overall phase formation by means of metastable phases. Such a metastable form of NAT is consistent with  $\alpha$ -NAT identified by Koehler *et al.* (32) and also observed by Iraci *et al.* in liquid  $\text{H}_2\text{SO}_4$  films (23).
  34. The only exception is experiment c in Fig. 3, when slow cooling led to the initial formation of metastable  $\alpha$ -NAT. However, even in that experiment the  $\alpha$ -NAT did not persist, with subsequent ice nucleation leading to metastable NAD.
  35. The current experiment is extremely sensitive to metastable phases. Detection of the vapor phase allows a gas-solid equilibrium to be maintained by a thin surface layer (tens of monolayers or less), minimizing the saturation ratios required for phase formation and growth. Metastable phases are easily detectable with our capability for long observation-equilibration times. Thus, our observations of sequential phases forming in the ternary system are not necessarily inconsistent with recent reports of direct NAT nucleation from the ternary liquid (22, 23). Those experiments detected relatively large crystals difficult to grow under equilibrium conditions.
  36. H. R. Pruppacher and J. D. Klett, *Microphysics of Clouds and Precipitation* (Reidel, Dordrecht, Netherlands, 1978), p. 714.
  37. D. Turnbull, *Metall. Trans. A* **124**, 695 (1981).
  38. In our experiments the mechanism of crystallization is unclear—that is, whether nucleation occurs heterogeneously on the substrate or homogeneously in the liquid. The same uncertainty exists for the stratospheric case. Our results imply that whatever the details, metastable phases dominate phase formation, consistent with the anticorrelation of nucleation barriers and crystal free energies predicted by Ostwald's rule.
  39. T. Peter, paper presented at the Heterogeneous Chemistry Workshop, Boulder, CO, 8 to 10 November 1993; M. A. Tolbert, *Science* **264**, 527 (1994); K. F. Carslaw *et al.*, *Geophys. Res. Lett.* **23**, 2479 (1994); K. Drdla *et al.*, *ibid.*, p. 2475.
  40. E. V. Browell *et al.*, *Science* **261**, 1155 (1993).
  41. Supported by the National Aeronautics and Space Administration: Upper Atmospheric Research Program, contract NASW 4126, and Atmospheric Effects of Aircraft Program, contract NAS1-19931, both to Aerodyne Research.

19 July 1994; accepted 5 October 1994

## Mechanisms of Argon Retention in Clays Revealed by Laser $^{40}\text{Ar}$ - $^{39}\text{Ar}$ Dating

Hailiang Dong, Chris M. Hall, Donald R. Peacor, Alex N. Halliday

A method for dating clays is important for studies of weathering, diagenesis, hydrocarbon migration, and the formation of major metalliferous deposits. However, many attempts have produced imprecise or inaccurate results. Data from shales show that, contrary to expectations, the  $^{40}\text{Ar}$ - $^{39}\text{Ar}$  dating technique can be successfully used to determine the diagenetic age of ancient sediments because  $^{39}\text{Ar}$  losses during irradiation are controlled by release from low retentivity sites in illite equivalent to those that have lost radiogenic  $^{40}\text{Ar}$  in nature, rather than by direct recoil as is generally assumed.

Formation of clays involved in weathering, diagenesis, or hydrothermal alteration has been difficult to study because such low temperature nonequilibrium processes are difficult to simulate experimentally. Clay mineral diagenesis has been variously ascribed to progressive temperature-induced formations (1), fluid mediated punctuated recrystallization (2, 3), and Ostwald ripening (4). In order to test these hypotheses, or establish the ages of diagenetic and hydrothermal reactions in nature, suitable isotopic dating methods must be developed for determining the timing of clay mineral growth. This has not been straightforward. The Rb-Sr approaches (2, 3) are generally limited by concerns over the uniformity of initial isotopic composition. Sm-Nd meth-

ods (3, 5) have similar problems and lack precision. K-Ar dating (6) is limited by the uncertainties of Ar loss. Furthermore, all of these techniques must utilize reasonably large samples ( $> 10$  mg).

The  $^{40}\text{Ar}$ - $^{39}\text{Ar}$  dating technique is a potentially powerful method for dating clay diagenesis and low-grade metamorphism because it can easily be applied to small samples and, with step-heating, allows one to see through the effect of Ar loss. However, despite early attempts (7, 8), it has long been known that during irradiation,  $^{39}\text{Ar}$  is lost from fine-grained samples such as clays (9–13), rendering the apparent ages meaningless. The recoil distance of  $^{39}\text{Ar}$  has been estimated to be  $0.08 \mu\text{m}$  (9), the same magnitude as the typical grain sizes of clay minerals (14). Comparisons with conventional K-Ar determinations (12) and experiments with quartz tube encapsulation

(15–17) indicate sizable losses of  $^{39}\text{Ar}$ , up to 60%, during irradiation. However, some comparisons between K-Ar and  $^{40}\text{Ar}$ - $^{39}\text{Ar}$  ages in fine-grained clay-like minerals yielded concordant results (12, 18–20), suggesting that under some circumstances,  $^{39}\text{Ar}$  loss due to recoil is negligible. Indeed, it has been inferred that the extent of  $^{39}\text{Ar}$  loss can be a function of the nature of clay grain boundaries and the relationships with neighboring grains (12, 18).

Illite, the most common K-rich clay mineral, commonly forms by diagenetic alteration of smectite, and in many sedimentary rocks, clays consist of mixed layers of these two minerals. Transmission electron microscopy (TEM) observations of illite-smectite (I-S) mixtures from mudstones (21) have revealed a positive correlation between the proportion of smectite-like layers and the relative proportions of imperfections in I-S crystallites. These imperfections may serve as pathways for radiogenic  $^{40}\text{Ar}$  diffusion loss in nature or the laboratory and  $^{39}\text{Ar}$  loss in the reactor. In this study we address the relation between the proportion of imperfections in I-S clays and the extent of Ar recoil-diffusion loss with a combination of TEM observations and vacuum encapsulation experiments on submilligram samples of clays.

We initially analyzed two bentonites and one shale from the classic Lower Paleozoic sedimentary successions of Wales. These horizons have well-established biostratigraphy and their depositional ages have been determined or bracketed by U-Pb zircon dating of bentonites (22). The shale has been independently studied using Rb-Sr and Sm-Nd techniques (5, 23). A similar experiment was performed on a well-characterized siltstone sample, also primarily studied by TEM, Rb-Sr, and Sm-Nd, from the Onondaga Group (Middle Devonian) of upper New York State. Bentonite sample RJM536 is from the Middle Cambrian Menevian Beds with a depositional age of 517 to 530 Ma (24). However, it was significantly metamorphosed during the Acadian orogeny at about 397 Ma (23), as indicated by its small illite crystallinity value of 0.17 (epizone). Bentonite sample BRM1311 is from the Upper Caradoc Formation (Ordovician) and has a depositional age range of 443 to 462 Ma (24). As opposed to RJM536, it is of low grade with an illite crystallinity (IC) of 0.84, corresponding to diagenetic grade. Three size fractions ( $5$  to  $1 \mu\text{m}$ ,  $1$  to  $0.2 \mu\text{m}$ , and  $<0.2 \mu\text{m}$ ) were obtained from the diagenetic shale collected from Pwllheli in the Welsh Basin. It has a depositional age within the range 461 to 449 Ma (5). The same size fractions were used for the diagenetic siltstone from New York. It has a maximum depositional age of  $390 \pm 1$  Ma (5) determined from

Department of Geological Sciences, University of Michigan, Ann Arbor, MI 48109–1063, USA.

U-Pb zircon dating of an underlying bentonite. As in the case of BRM1311, these two samples have large illite crystallinity values corresponding to diagenetic grade.

Powder diffractometer data were obtained and scanning electron microscopy and TEM observations (25) were made for each sample used for  $^{40}\text{Ar}$ - $^{39}\text{Ar}$  analysis. The bentonites and Welsh shale were studied using two  $^{40}\text{Ar}$ - $^{39}\text{Ar}$  techniques. In the first, the aliquot was simply wrapped in Al foil and packed with others into evacuated quartz tubes for irradiation. In the second, the aliquot was encapsulated under high vacuum ( $10^{-8}$  torr) in a pure quartz ampoule in order to capture any gas lost during irradiation and hence determine an age equivalent to that of conventional K-Ar dating (27, 28). One aliquot was also dated by the conventional K-Ar technique as a check on this procedure. The irradiated quartz ampoules were broken under high vacuum, and the freely released gases measured first, followed by normal step-heating using a continuous Ar ion laser (Table 1 and Fig. 1). The proportion of  $^{39}\text{Ar}$  that escaped from the clay during irradiation and was captured in the quartz ampoule varied significantly among the samples (Table 1).

The middle Cambrian metamorphosed bentonite, sample RJM536, is dominated by well-crystallized illite (>85%) with small proportions of calcite and pyrite (Fig. 1A). TEM images (Fig. 1B) and XRD patterns show that it consists of illite with no expandable component (29). The layers occur in well-defined packets of less than 1  $\mu\text{m}$  thickness with no observable dislocations (layer terminations). Analytical electron microscopy (AEM) data

show that the illite has a K content of 0.7 to 0.8 per 11 O atoms, consistent with immature illite. This sample released only 0.8 to 0.9% of its  $^{39}\text{Ar}$  during irradiation. The integrated and plateau ages for the aliquot with no vacuum encapsulation are almost identical to those of the encapsulated aliquot (Table 1). The age spectra (Fig. 1C) are suggestive of diffusive loss of  $^{40}\text{Ar}$ , but all these analyses show well-defined plateaus, similar to the results of Bray *et al.* (20). Based on a model of slow cooling, the plateau age of 416 to 420 Ma might represent the peak of metamorphism, and the integrated age of about 399 Ma the time when the K-Ar system became closed. For an assumption of rapid cooling, the plateau age probably reflects the peak of metamorphism, and the total gas age would reflect partial resetting by a later thermal event.

In contrast, the Ordovician bentonite, sample BRM1311 consists of illite and I-S (70%), quartz (10%), chlorite (15%) and some muscovite (Fig. 1D). TEM images show that illite and I-S occur as randomly distributed packets with thicknesses of 50 to 100  $\text{\AA}$  (Fig. 1E). The packets intersect at acute angles, resulting in abundant voids at boundaries. This is the only sample that contains a significant proportion of smectite layers in I-S (20%) as determined from both XRD and TEM. The total gas ages for the unencapsulated aliquot are much older than the depositional age (Table 1). The  $^{39}\text{Ar}$  loss is 27.2 to 31.7% of the total for the encapsulated samples, and the encapsulated total gas ages (equivalent to K-Ar ages) are almost 100 million years younger than the depo-

sitional age (Fig. 1F and Table 1). However, if the  $^{39}\text{Ar}$  loss is subtracted from the total, integration of the remaining gas fractions yields poorly reproducible ages close to but still slightly higher than the known depositional age (Table 1). As these ages were obtained from  $^{40}\text{Ar}$  and  $^{39}\text{Ar}$  atoms retained in the mineral at room temperature, they are referred to as "retention ages."

The Welsh Ordovician shale sample is distinct from both bentonites and composed of illite, chlorite, muscovite, quartz and pyrite (Fig. 1G). TEM images show that illite packets 40 to 200  $\text{\AA}$  thick alternate with chlorite packets 200 to 1000  $\text{\AA}$  thick (Fig. 1H). However, when the whole rock was crushed, and the different size fractions separated, this texture was disarticulated. Chlorite peaks were not present in XRD patterns of the <0.2- $\mu\text{m}$  size fraction, suggesting that the large chlorite packets were removed from this finest size fraction. As a result, the illite packets were isolated from each other, and the space between such packets is equivalent to voids or dislocations. The integrated ages for the unencapsulated aliquot of the <0.2- $\mu\text{m}$  fraction are consistent with the depositional age (Table 1), and the older age of the 1- to 5- $\mu\text{m}$  size fraction is attributed to a detrital component. However, the encapsulated total gas ages (equivalent to K-Ar ages) are much younger than the depositional age (Table 1), and apparently geologically meaningless. The  $^{39}\text{Ar}$  losses for these three fractions are in the range of 10.7 to 28.0%, and the finest fraction yielded the greatest  $^{39}\text{Ar}$  loss (Fig. 1I and Table 1). In this case, following subtraction of the  $^{39}\text{Ar}$  loss from the total, the resulting retention

**Table 1.**  $^{40}\text{Ar}$ - $^{39}\text{Ar}$  ages of bentonites and shales. All uncertainties are  $\pm 2\sigma$ .

Sample	Illite crystallinity* ( $\Delta 2\theta$ )	Depositional age (Ma)	Unencapsulated total gas age (Ma)	Encapsulated total gas age (Ma)	Retention age (Ma)	Rb-Sr age (Ma)	Encapsulated % $^{39}\text{Ar}$ loss
<i>Bentonite (Wales)</i>							
RJM536	0.17	517-530	407.2 $\pm$ 1.6 412.2 $\pm$ 1.7	397.9 $\pm$ 1.5 400.8 $\pm$ 1.8	404.9 $\pm$ 0.6 401.1 $\pm$ 0.8		0.99 0.82
BRM1311	0.84	443-462	535.5 $\pm$ 1.8 536.5 $\pm$ 1.9	350.2 $\pm$ 1.4 347.9 $\pm$ 1.6	465.6 $\pm$ 1.2 489.7 $\pm$ 1.1		27.24 31.73
<i>Shale (Wales)</i>							
1 to 5 $\mu\text{m}$	0.45	449-461	481.9 $\pm$ 2.4	418.8 $\pm$ 2.2	463.6 $\pm$ 1.3		10.65
0.2 to 1 $\mu\text{m}$	0.52	449-461	477.2 $\pm$ 1.8 464.6 $\pm$ 2.0	371.9 $\pm$ 1.9 392.9 $\pm$ 2.4	453.0 $\pm$ 1.3 448.6 $\pm$ 1.1		19.60 13.73
<0.2 $\mu\text{m}$	0.78	449-461	454.2 $\pm$ 3.6 458.2 $\pm$ 2.8	323.5 $\pm$ 1.6 326.0 $\pm$ 2.1	428.0 $\pm$ 1.4 435.1 $\pm$ 1.3	430 $\pm$ 5	25.97 27.97
<i>Siltstone (New York)</i>							
1 to 5 $\mu\text{m}$	0.40	390 $\pm$ 1		452.2 $\pm$ 3.7	498.0 $\pm$ 0.8		10.50
0.2 to 1 $\mu\text{m}$	0.42	390 $\pm$ 1		423.0 $\pm$ 2.5 425.5 $\pm$ 4.2	477.1 $\pm$ 1.0 472.1 $\pm$ 2.6		12.66 10.93
<0.2 $\mu\text{m}$	0.60	390 $\pm$ 1		341.4 $\pm$ 1.8 354.2 $\pm$ 1.3	423.1 $\pm$ 0.6 426.3 $\pm$ 0.6	410 $\pm$ 4	21.18 18.69

\*Illite crystallinity, IC >0.43, 0.43-0.26, and <0.26 correspond to the diagenetic, the anchizone, and epizone grade, respectively.

ages for the  $<0.2 \mu\text{m}$  fraction are reproducible and close to the depositional age, and the ages for the unencapsulated samples

(Table 1) and identical to a Rb-Sr leachate-residue age of  $430 \pm 5 \text{ Ma}$  for the same clay size fraction (5).

The equivalence of the vacuum-encapsulated results and those of the conventional K-Ar method was verified by a K-Ar age

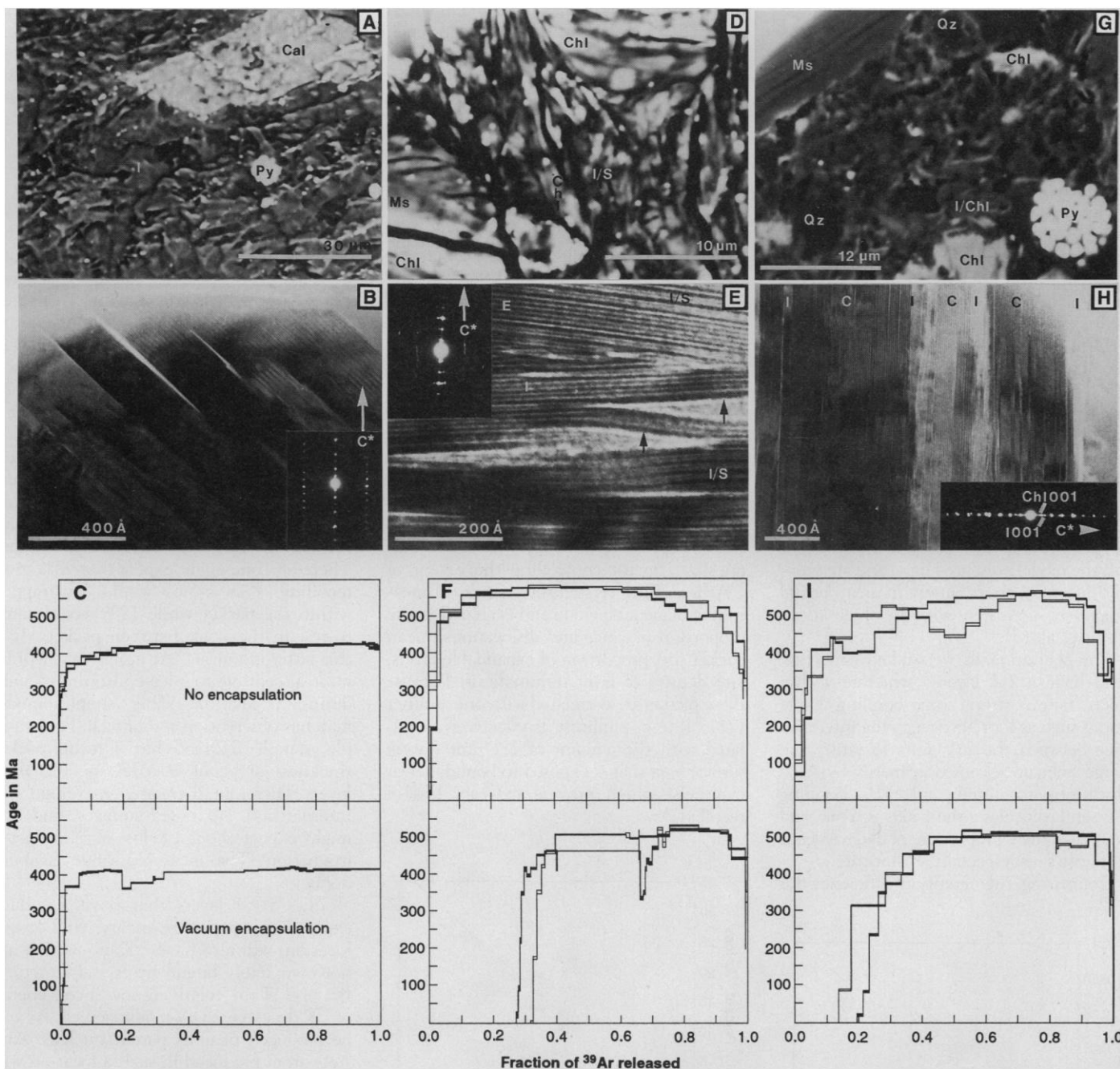


**Fig. 1.** Scanning and transmission electron microscopy images and age spectra for samples BRM1311, RJM536, and 0.2 to  $1 \mu\text{m}$  size fraction of the shale. **(A)** Back-scattered electron image of sample RJM536. Cal, calcite; I, illite; Py, pyrite. **(B)** TEM lattice fringe image and selected area electron diffraction (SAED) pattern of sample RJM536 showing dislocation-free, well-ordered 2M, illite of mean packet thickness of 1000 Å. These features are responsible for the negligible  $^{39}\text{Ar}$  loss. **(C)** Age spectra for sample RJM536. Both unencapsulated and encapsulated runs yielded plateau ages of 416 to 420 Ma. The decrease in the apparent age is caused by uneven heating by the laser as a result of one clump shadowing the other. **(D)** BSE image of BRM1311. Chl, chlorite; I/S, illite/smectite; Ms, muscovite. **(E)** TEM lattice fringe image BRM1311 showing abundant voids, dislocations and layer terminations at small angle-like boundaries of I-S (illite) packets, and the corresponding SAED pattern showing disorder and variable layer orientation. The voids and dislo-

cations account for the high degree of  $^{39}\text{Ar}$  loss. **(F)** The disturbed age spectra, as a result of  $^{39}\text{Ar}$  redistribution, of both unencapsulated and encapsulated runs for sample BRM1311. **(G)** BSE image of the whole rock shale. Chl, chlorite; I, illite; I/Chl, illite/chlorite; Ms, muscovite; Py, pyrite; Qz, quartz. **(H)** TEM lattice fringe image and the corresponding SAED pattern of the whole rock shale showing that illite (I) packets 50 to 200 Å thick alternate with chlorite (C) packets 200 to 1000 Å thick. These small illite packets were isolated from one another and from chlorite packets during separation, and the space between the isolated illite packets to the voids and dislocations in the case of sample BRM1311, resulting in disturbed age spectra and enhanced  $^{39}\text{Ar}$  loss. **(I)** The disturbed age spectra of 0.2- to  $1\text{-}\mu\text{m}$  size fraction. The K-Ar age of  $387 \pm 7 \text{ Ma}$  is identical to the encapsulated ages, demonstrating that the encapsulated results are truly equivalent to those of the K-Ar method.

( $387 \pm 7$  Ma,  $2\sigma$ ) of one size fraction (0.2 to  $1 \mu\text{m}$ ) of the Welsh shale. This demonstrates that the total gas ages for encapsulated samples are truly equivalent to K-Ar ages and are not an artifact of some aspect of the experiment. The young K-Ar ages of the clay-rich samples relative to the depositional age indicate that radiogenic  $^{40}\text{Ar}$  has been lost, probably in nature. However, the similarity between the measured retention age and Rb-Sr age in the Welsh shale strongly suggests that the  $^{39}\text{Ar}$  loss that occurred in the reactor is correlated with the radiogenic  $^{40}\text{Ar}$  loss. That is, the sites of preferential low-temperature loss must have been similar for both  $^{40}\text{Ar}$  and  $^{39}\text{Ar}$  atoms. This conclusion is verified by a good agreement between the depositional age, retention age, and the leachate-residue Rb-Sr age for the  $<0.2\text{-}\mu\text{m}$  size fraction of the siltstone from New York (Table 1). This rock is composed of muscovite, illite, chlorite, quartz, and calcite, and is comparable to the Welsh shale. The proportion of the detrital component decreases from the coarsest to the finest fraction, but some detrital material is still present in the  $<0.2\text{-}\mu\text{m}$  fraction, as detected by XRD. Therefore, the slightly old retention and Rb-Sr ages for the  $<0.2\text{-}\mu\text{m}$  fraction relative to the depositional age are not inconsistent with the model presented here, and are probably due to a contribution from a detrital component, consistent with the observations of Ohr et al. (5).

The clay minerals we studied (smectite, illite) have a 2:1 layered structure within which there is strong ionic bonding. Large cations such as K or Na occupy the interlayer space between the 2:1 units to satisfy the charge imbalance caused primarily by  $\text{Al}^{3+}$  substitution for tetrahedral  $\text{Si}^{4+}$ . Bonding between layers along the *c* axis is weak, and there is a high proportion of large vacant interlayer sites, especially in smectite.

Comparing the retention efficiency for

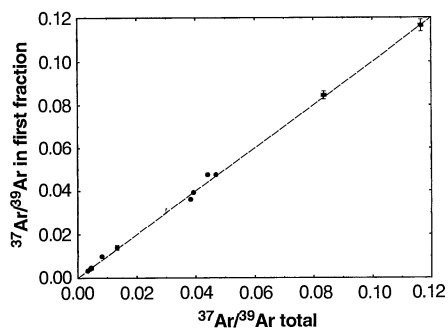


**Fig. 2.**  $^{37}\text{Ar}/^{39}\text{Ar}$  in first fraction (freely released gas) versus  $^{37}\text{Ar}/^{39}\text{Ar}$  of the total gas showing that these two ratios are virtually identical. The 1:1 reference line is for comparison. Error bars are  $1\sigma$ . The data points for sample RJM536 and 1- to  $5\text{-}\mu\text{m}$  size fraction of the New York siltstone are not included because these two samples have a significant proportion of calcite.

Ar nuclei with different recoil energies provides some insights into how the clay structure accommodates Ar atoms. The mean recoil distance for  $^{37}\text{Ar}$  has been calculated to be over twice that of  $^{39}\text{Ar}$  (9, 17) which, for isolated grains, would result in enhanced  $^{37}\text{Ar}$  recoil loss compared to  $^{39}\text{Ar}$ . However, our data (Fig. 2) confirm the finding of Smith et al. (17) that the  $^{37}\text{Ar}/^{39}\text{Ar}$  ratio in the recoil gas is essentially the same as that in the bulk sample. They proposed that the implantation of recoiling atoms into neighboring glauconite pellets is independent of the initial energy of the recoiling atoms, but is instead dependent on the energy remaining before the last impact with a clay packet. This energy was calculated to be the same for both  $^{37}\text{Ar}$  and  $^{39}\text{Ar}$ , thereby leading to the same ratio in the recoil gas as in the rest of the sample. This model is also compatible with the observation that recoil loss correlates well with surface to volume ratio (18). Therefore it appears that surface interactions with recoiling atoms play an important role in determining the extent of Ar loss.

The strong correlation between the measured illite crystallinity and the percentage of  $^{39}\text{Ar}$  loss during irradiation (Fig. 3) suggests that the amount of the layer surface that is exposed to illite (I-S) packet boundaries is a factor controlling the extent of  $^{39}\text{Ar}$  loss. Illite crystallinity is a direct measure of diagenetic grade and is related to the proportion of voids and dislocations, mean packet size, proportion of expandable layers, and density of layer terminations. Because these factors are correlated with one another (21), illite crystallinity is effectively correlated with the amount of 2:1 unit (layer) surface area that is exposed to boundaries or channels, which provide for easy loss of recoiled Ar.

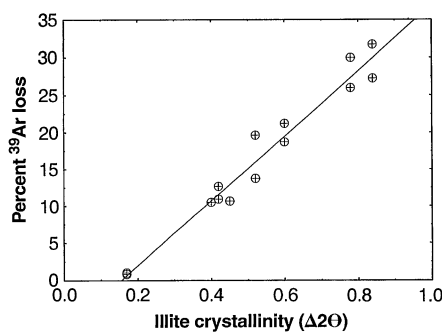


**Fig. 3.** For the shale fractions and sample RJM536, illite crystallinity is effectively a measure of packet size. For BRM1311, it is a measure of both packet size and smectite proportion. The strong correlation between  $^{39}\text{Ar}$  loss and illite crystallinity indicates that the extent of  $^{39}\text{Ar}$  loss is apparently determined by illite crystallinity, that is, proportions of voids and dislocations, mean packet size, density of dislocations, and state of disorder. Least squares fit through the data. Percent  $^{39}\text{Ar}$  loss =  $43.8(\Delta 2\theta) - 6.74$ ,  $R^2 = 0.962$ .

For sample RJM536, the illite crystallinity is 0.17, corresponding to well-crystallized and dislocation-free illite of large mean crystal thickness ( $1000 \text{ \AA}$ ), and  $^{39}\text{Ar}$  loss was negligible. However, for the other samples, illite crystallinities are in the range of 0.40 to 0.84, corresponding to variable but high proportions of dislocations, small mean packet thickness ( $100 \text{ \AA}$  or less) and expandable layers. The large losses of  $^{39}\text{Ar}$  from these samples are therefore ascribed to the dislocations and voids, which provide abundant pathways for  $^{39}\text{Ar}$  loss.

We envisage that it is necessary for a recoiled atom ( $^{39}\text{Ar}$  or  $^{37}\text{Ar}$ ) to traverse at least one layer in order to be retained in the crystal structure. Each 2:1 unit (layer) can be viewed as having two surfaces that have  $\text{K}^+$  ions attached, and the interlayer area would then have  $\text{K}^+$  ion contributions from two adjoining layers. A hypothetical  $100 \text{ \AA}$  clay packet should consist of 10 layers, each having two surfaces. Of the total of 20 surfaces in the packet, 18 (90%) are internal and 2 (10%) are exposed and weakly bonded. Any of these surfaces, either internal or exposed, is an equally likely resting place for a recoiling atom, provided that there are no losses of energy in the voids because of collisions with gas molecules. Therefore, one might expect that 90% of all recoiling  $^{39}\text{Ar}$  atoms would be trapped within the packet while 10% would come to rest in the voids between packets. It is this latter group of  $^{39}\text{Ar}$  atoms that will be most susceptible to release into the vacuum during irradiation. This simple model matches observation rather well. For example, sample RJM536 has a mean packet thickness of about  $1000 \text{ \AA}$ , or 100 illite layers. Therefore, there are, on average, 198 internal and 2 exposed surfaces, and one might expect about 1% loss of  $^{39}\text{Ar}$  during irradiation. The measured value is about 0.9%.

Illite (I/S) layers that have a surface exposed to a packet boundary, void or dislocation, will also have  $^{40}\text{K}$  atoms that are not completely bound by crystal structure. Because of the relatively low recoil energy of  $^{40}\text{K}$  decay ( $\sim 28 \text{ eV}$ ), radiogenic  $^{40}\text{Ar}$  will be produced near its parent nucleus. Any  $^{40}\text{Ar}$  atom produced in such a location will be highly vulnerable to loss. In the case of pure illite packets, the K concentration at the exposed surfaces is the same as that at the internal surfaces. Therefore, if the mean packet thickness is about  $100 \text{ \AA}$  (that is, 2 surfaces out of 20 are exposed to voids), 10% of the total  $^{40}\text{Ar}$  produced will be in such low-retentivity sites. The concordance between the Ar retention ages and the known depositional ages of these samples suggests that the probability of retention of either  $^{40}\text{Ar}$  produced by in situ decay or  $^{39}\text{Ar}$  produced by neutron reaction is equal,

to a first approximation. Thus, the retentive sites are the chronometer of the time of diagenetic mineral growth or Ar closure. This conclusion is consistent with the model by Thompson and Hower (30) that the proportion of exchangeable K must be subtracted from the total to obtain a correct K-Ar age (depositional).

Because the recoil distance of  $^{39}\text{Ar}$  is large compared with the mean packet thickness for clay samples, the  $^{39}\text{Ar}$  concentration during irradiation is effectively homogenized throughout the sample. However, any  $^{39}\text{Ar}$  that comes to a rest at a nonretentive site will be quickly released into the evacuated capsule. If the K concentration of retentive and nonretentive sites is the same, as in the case of Welsh shale and New York siltstone, the  $^{39}\text{Ar}/\text{K}$  ratio in the retentive sites should be the same as that for the irradiation monitor mineral. Thus, the measured retention age would be expected to give the best estimate for the time of Ar blocking. This blocking age represents either the depositional-diagenetic age (in the case of BRM1311, Welsh shale and New York siltstone), or metamorphic age (in the case of RJM536), depending on the metamorphic grade. However, if the voids and packet boundaries that constitute the nonretentive sites are rich in K-poor smectite layers, as in the case of BRM1311, or if K has been partially stripped out from these nonretentive sites before sampling, the recoil-induced homogenization of  $^{39}\text{Ar}$  should produce a decrease in the  $^{39}\text{Ar}/\text{K}$  ratio for the retentive sites, and the retention age will be an overestimate of the age of Ar blocking in the clays. In the extreme case where all K in nonretentive sites has been stripped out, all  $^{40}\text{Ar}$  and K would reside in retentive sites only, and the homogenization of  $^{39}\text{Ar}$  by recoil would lead to an erroneously high Ar retention age. It would be theoretically possible to correct the measured retention age for those samples that have a significant proportion of smectite layers or have partially or completely lost K from nonretentive sites if a precise distribution of K in nonretentive and retentive sites were known. This information is not currently available. However, in the case that the K has been completely stripped out from nonretentive sites, the corrected retention age would be expected to be the same as the encapsulated total gas age. This model is similar to the conclusion of Aronson and Douthitt (31) who studied Ar retention in acid-leached clays. Our procedure allows us to obtain both the total gas and the Ar retention ages.

The total gas age for the unencapsulated aliquot is systematically older than the corresponding retention age for the encapsulated aliquot for all the samples (Table 1).

In particular, the total gas age for the unencapsulated aliquot of sample BRM1311 is almost 100 million years older than the retention age for the encapsulated aliquot. The difference between these two ages may be related to the difference in pressure to which the two aliquots were subjected. The unencapsulated and encapsulated aliquots were irradiated at pressures of approximately  $10^{-3}$  to  $10^{-4}$  and  $10^{-7}$  to  $10^{-8}$  torr, respectively. Smith *et al.* (17) demonstrated that low pressures could significantly reduce the extent of  $^{39}\text{Ar}$  recoil loss. The different behavior for sample BRM1311 is presumably because of its high concentration of smectite (20%).

The encapsulated  $^{40}\text{Ar}$ - $^{39}\text{Ar}$  step-heating experiments effectively sample a broad range of Ar retention sites. It might not be expected that the loss mechanisms for  $^{40}\text{Ar}$  and  $^{39}\text{Ar}$  should be identical through this entire range. The age spectra for the shale separates plus the BRM1311 bentonite (Figs. 1, F and I) reveal high apparent ages in the middle of the Ar release and low apparent ages at both low and high temperatures. This indicates that the distribution of  $^{39}\text{Ar}$  and  $^{40}\text{Ar}$  was not uniform in retentive sites.  $^{39}\text{Ar}$  atoms were clearly able to recoil into some sites in which  $^{40}\text{Ar}$  was not highly concentrated. The release of Ar from these sites in the laboratory has nothing to do with the loss of  $^{40}\text{Ar}$  in nature, which complicates the detailed interpretation of age spectra.

Radiogenic  $^{40}\text{Ar}$  is preferentially lost from the same kinds of low retentivity sites that are responsible for the loss of neutron-introduced  $^{39}\text{Ar}$ . Loss of  $^{39}\text{Ar}$  during irradiation is caused more by the retentivity of the  $^{39}\text{Ar}$  atom's final destination than by direct ejection from the sample. Therefore for those clay samples whose K-Ar system has been partially reset in geological history, the Ar retention age is most likely to represent a better estimate of the time of mineral growth.

## REFERENCES AND NOTES

- J. Hower, E. V. Eslinger, M. H. Hower, E. A. Perry, *Geol. Soc. Am. Bull.* **87**, 725 (1976).
- J. P. Morton, *ibid.* **96**, 114 (1985).
- M. Ohr, A. N. Halliday, D. R. Peacor, *Earth Planet. Sci. Lett.* **105**, 110 (1991).
- D. D. Eberl, J. Srodon, M. Kralik, B. E. Taylor, Z. E. Peterman, *Science* **248**, 474 (1990).
- M. Ohr, A. N. Halliday, D. R. Peacor, *Geochim. Cosmochim. Acta.* **58**, 289 (1994).
- J. L. Aronson and J. Hower, *Geol. Soc. Am. Bull.* **87**, 738 (1976).
- I. A. Cowperthwaite, F. J. Fitch, J. A. Miller, J. G. Mitchell, R. H. S. Robertson, *Clay Mineral.* **9**, 309 (1972).
- K. C. Dunham, F. J. Fitch, P. R. Ineson, J. A. Miller, J. G. Mitchell, *Proc. R. Soc. London Ser. A* **307**, 251 (1968).
- G. Turner and P. H. Cadogan, *Proc. Lunar Sci. Conf.* **5**, 1601 (1974).
- J. C. Huneke and S. P. Smith, *Geochim. Cosmochim. Acta.* (Suppl.) **7**, 1987 (1976).
- Y. Yanase, J. M. Wampler, R. E. Dooley, *Eos* **56**, 472 (1975).
- A. N. Halliday, *Geochim. Cosmochim. Acta.* **42**, 1851 (1978).
- K. A. Foland, J. S. Linder, T. E. Laskowski, K. Grant, *Chem. Geol.* **46**, 241 (1984).
- R. J. Merriman and B. Roberts, *Mineral. Mag.* **49**, 305 (1989).
- J. C. Hess and H. J. Lippolt, *Chem. Geol.* **59**, 223 (1986).
- K. A. Foland, F. A. Hubacher, G. B. Aehart, *ibid.* **102**, 269 (1992).
- P. E. Smith, N. M. Evensen, D. York, *Geology* **21**, 41 (1993).
- A. Reuter and R. D. Dallmeyer, *Contrib. Mineral. Petrol.* **97**, 352 (1987).
- P. M. Vasconcelos, T. A. Becker, P. R. Renne, G. H. Brimhall, *Geochim. Cosmochim. Acta.* **58**, 1635 (1994).
- C. J. Bray *et al.*, *Can. J. Earth Sci.* **24**, 10 (1987).
- D. R. Peacor, in *Minerals and Reactions at the Atomic Scale: Transmission Electron Microscopy, Reviews in Mineralogy*, vol. 27, P. R. Buseck, Ed. (Mineralogical Society of America, Washington, DC, 1992), pp. 335-380; J. H. Ahn and D. R. Peacor, *Clays Clay Minerals* **34**, 165 (1986b).
- R. D. Tucker, T. E. Krogh, R. J. Ross, S. H. Williams, *Earth Planet. Sci. Lett.* **100**, 51 (1990).
- J. A. Evans, *J. Geol. Soc. London* **148**, 703 (1991).
- W. R. Harland *et al.*, in *A Geologic Time Scale* (Cambridge Univ. Press, Cambridge, 1989), pp. 33-35.
- The two bentonites and Welsh shale whole-rock samples were expanded with L R White resin following the procedure of (26) so that the smectite and illite layers are easily distinguished in TEM images, allowing direct observation of the proportion of expandable layers in mixed layer I-S clays. Sticky-wax-backed thin sections were prepared, followed by examination of optical microscopy and scanning electron microscopy to obtain textural relationship between various mineral phases. Typical areas that contain phyllosilicates were removed from thin sections for TEM observations via attached Al washers, thinned and carbon-coated.
- J. W. Kim, D. R. Peacor, D. Tessier, F. Elsass, *Clays Clay Minerals*, in press.
- Because earlier trials had indicated that release of gas began at low temperatures in these samples, the quartz ampoules were sealed while their bottoms were immersed in water to ensure that the sample grains were kept at room temperature; the tops were then heated in order to detach them from the manifolds. These 4- to 5-cm quartz ampoules were then seated inside quartz sleeves wrapped in pure Al foil. The wrapped sleeves were then loaded into large quartz tubes with the sleeves alternating with mmhb-1 hornblende standards (28). The quartz tubes were sealed in a vacuum of  $10^{-4}$  torr and then immersed in a large water bath under partial vacuum to test for leakage. Assemblies of quartz tubes were set inside quartz boats and dropped in position L75 of the Phoenix Ford Memorial Nuclear Reactor for irradiation for 60 hours at a power level of 2 MW. After irradiation, the quartz tubes were opened and the quartz ampoules were transferred inside pyrex sleeves. The pyrex sleeves were set inside pyrex tubes followed by attachment of these tubes to manifolds for analysis.
- S. D. Samson and E. C. Alexander, *Chem. Geol.* **66**, 27 (1987).
- The proportions of the expandable component (smectite) in I-S clays were determined by comparison of XRD patterns of air-dried material with those of the same samples saturated with ethylene glycol.
- G. Thompson and J. Hower, *Geochim. Cosmochim. Acta* **37**, 1473 (1973).
- J. L. Aronson and C. B. Douthitt, *Clays Clay Minerals* **34**, 473 (1986).
- We thank R. J. Merriman, B. Roberts, M. Ohr, and N. C. Ho for help in collecting samples, M. Johnson for technical support, and W. C. Elliott for K-Ar analysis. We thank three reviewers for their comments. This research was supported in part by NSF grants to D.R.P., C.M.H., and A.N.H. and by the Michigan Memorial Phoenix Project.

22 September 1994; accepted 12 December 1994